JOURNAL OF CATALYSIS 92, 388–397 (1985)

Investigation of Interactions between Metals and Adsorbed Organic Compounds by Infrared Spectroscopic Study of Adsorbed CO

III. Production of Desorption–Adsorption Infrared Doublet of CO on Pt/Cab-O-Sil and Interaction of Adsorbed CO with Hydrogen and Oxygen

JÁNOS SÁRKÁNY AND MIHÁLY BARTÓK

Department of Organic Chemistry, József Attila University, Szeged, H-6720, Hungary

Received May 11, 1984; revised November 19, 1984

The possibilities of formation of the CO infrared absorption doublet were examined by transmission infrared spectroscopy, in the frequency interval for CO chemisorbed in linear form (2100–2000 cm^{-1}) on variously treated 5% Pt/Cab-O-Sil catalysts. The resolution of the doublet at about 2070 and 2050 cm^{-1} was not very good for a freshly reduced sample. Treatment in CO or O_2 promoted formation of the doublet, whereas surface hydrogen completely inhibited it. A CO doublet could not be produced on a sample which had been used several times in CO + O_2 reaction cycles. The surface CO layers relating to the CO doublet exhibited different reactivities toward O_2 at 298 K. In separate runs, in response to 10 Torr H_2 at 298 K, the position of the low-frequency (desorptive) CO band shifted from 2052 to 2061 cm^{-1}, while that of the high-frequency (adsorptive) band underwent a red shift, from 2072 to 2068 cm^{-1}. © 1985 Academic Press, Inc.

INTRODUCTION

We earlier reported (*1*) that the adsorption–desorption hysteresis in the CO frequency vs CO absorbance may be utilized to produce a desorptive–adsorptive CO ir doublet in the frequency range of linearly adsorbed CO on Pt/SiO_2. In the present work we have shown that the surface conditions of the self-supporting samples may influence the possibility of producing this doublet. We have attempted to gain a clearer picture of the properties of the adsorbed CO layers relating to the doublet, and the interactions of these with oxygen and hydrogen.

EXPERIMENTAL

Materials. The 5 wt% Pt/Cab-O-Sil catalyst was prepared by impregnation as before (*1*), when the gases (CO, H_2, and O_2) used in this study were also described.

Apparatus and procedure. Infrared spectra were recorded at room temperature with a double-beam Specord 75 ir spectrometer (Zeiss, Jena), generally at a rate of 1.36 cm^{-1} s^{-1}. The reproducibility in the frequency interval of interest was ±0.5–1 cm^{-1}. The ir cell (as in (*1*)) was connected to a conventional vacuum and gas-handling system, the ultimate pressure being 10^{-7} Torr (1 Torr = 133.3 N m^{-2}).

Preparation of the sample (with an optical density of 10 mg cm^{-2}) from the dried catalyst, and the standard pretreatment *in situ*, were described in detail previously (*1, 2*). Any variations in procedure have been indicated in the text. The results obtained from O_2 and CO chemisorption, measured with a Cahn vacuum-microbalance, gave Pt dispersities of 0.36 and 0.30 for reduced catalyst samples 1 and 2, respectively.

RESULTS

1. *Effect of Pretreatment on Formation of CO ir Absorption Doublet*

Following CO adsorption at 298 K on catalysts treated in various ways, partial thermal desorption was carried out under vacuum at 593–643 K to produce desorptive CO with appropriate intensity and frequency (ca. 2049–2052 cm^{-1}). Next (or af-

0021-9517/85 $3.00
Copyright © 1985 by Academic Press, Inc.
All rights of reproduction in any form reserved.

ter H_2 adsorption), CO was adsorbed in small doses onto the sample at 298 K (adsorptive CO). In some cases the two CO bands could be well distinguished (Figs. 1B and C), whereas in others the difference was poorer (Fig. 1A) or could not be observed at all (Figs. 1D, E, and F). With these exceptions, the resolution of the ir doublet was better if the relative change in intensity of the desorptive CO [A(D)/A(D,o)] in the course of CO adsorption was lower (Table 1).

2. *Effect of Hydrogen on Adsorbed CO at 298 K*

(a) Desorptive CO + H_2 (Fig. 2A). If hydrogen was adsorbed besides desorptive CO, the CO absorbance decreased. On admission of a dose of 7.5×10^{-3} Torr H_2, the CO frequency [ν(CO)] fell from 2052 to 2050 cm^{-1} (spectrum *b*); however, it was surprising that the admission of larger doses of H_2 led to increases: for 7.5×10^{-2} Torr H_2 ν(CO) was 2056 cm^{-1}, and for 10 Torr H_2 it was 2061 cm^{-1} (spectra *d* and *f*). Conversely, if the weakly bound hydrogen was removed by evacuation at 298 K ν(CO) fell to 2050 cm^{-1}; the absorbance increased markedly, but did not attain the initial value, while the band remained a little broader than it was at first (Fig. 2A, spectra, *a*, *g*, and *h*). The surface illustrated by spectrum *h* is very similar to that in Fig. 1D, spectrum *a*, where production of the CO ir doublet was unsuccessful.

(b) Adsorptive CO + H_2 (Fig. 2B). When H_2 was adsorbed besides adsorptive CO, the frequency and absorbance of the CO band decreased only slightly, even in the case of 100 Torr H_2. Evacuation for 10 min at 298 K caused the CO absorbance and frequency to increase, but the original values were not recovered.

If CO was adsorbed at 298 K on hydrogen-precovered Pt/SiO_2, similar results were obtained as on the interaction of preadsorbed CO (adsorptive CO) and H_2. The effects of H_2 on adsorbed CO are summarized in Table 2.

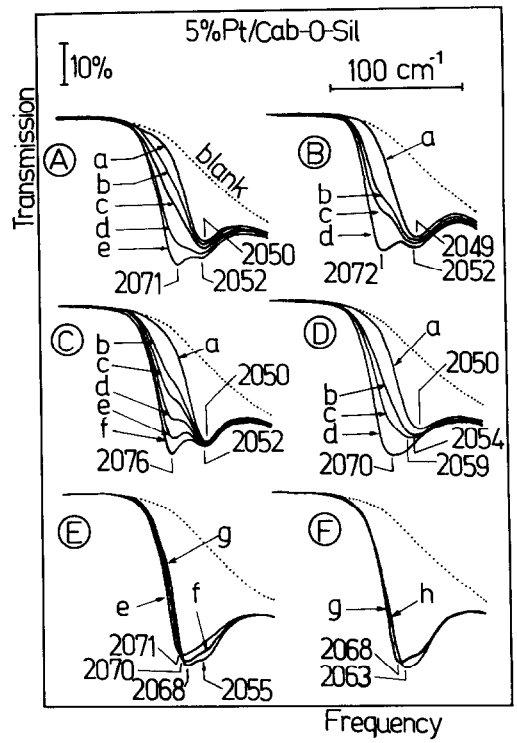

FIG. 1. Production of CO ir absorption doublet on variously treated catalyst. (A) Sample freshly reduced by standard pretreatment of newly prepared catalyst. (B) Sample used in five CO ad-and desorption cycles after the usual O_2–H_2 pretreatment. (C) After standard pretreatment, the freshly reduced catalyst was treated with CO; 10 Torr CO adsorption at 298 K for 30 min, heating in CO to 643 K, a 5-min waiting period and partial thermodesorption under vacuum at 643 K (desorptive CO). (D) 10 Torr H_2 was admitted for 5 min at 298 K to desorptive CO produced as in (C), followed by evacuation for 10 min at 298 K. Desorptive CO: (A, *a* and B, *a*) 10 Torr CO adsorption at 298 K for 10 min, then thermal desorption under constant evacuation at 593–643 K until appropriate band intensity; (C, *a*) see (C) above, and (D, *a*) 10 Torr H_2 was admitted for 5 min at 298 K to desorptive CO produced as in (C), followed by evacuation for 10 min at 298 K. From (*b*) to (*f*), stepwise CO adsorption at 298 K until appropriate band intensities of adsorptive CO (θ_{CO} around 0.3). [After each CO dose (from 10^{-4} to 10^{-2} Torr) a 5-min adsorption period was allowed before recording.] (E) and (F) after (D, *d*); (*e*) evacuation at 298 K for 10 min, then for 5 min each at (*f*) 373 K, (*g*) 398 K, and (*h*) 433 K.

3. *Attempt to Produce CO ir Doublet on Catalyst Used in CO + O_2 Reaction*

A considerable transformation is known

TABLE 1

Production of CO ir Absorption Doublet on Variously Treated 5% Pt/Cab-O-Sil Catalysts

Catalyst No.	Experimental conditions	Spectra from Figs. 1A, B, C, and D	Absorbance[a] $A = \log (T_0/T)_{max}$			$\frac{A(D,o)}{A(\theta = 1)}$	$\frac{A(D)}{A(D,o)}$
			$A(\theta = 1)$	$A(D,o)$	$A(D)$		
1	See Fig. 1A	A (a)		0.127		0.173	
		A (e)			0.167		1.31
	At $\theta_{CO} = 1$	—	0.733				
2	See Fig. 1B	B (a)		0.138		0.218	
		B (d)			0.160		1.16
	At $\theta_{CO} = 1$	—	0.634				
1	See Fig. 1C	C (a)		0.153		0.205	
		C (f)			0.164		1.07
	At $\theta_{CO} = 1$	—	0.746				
1	See Fig. 1D	D (a)		0.136		0.226	
		D (c) or (d)					
	At $\theta_{CO} = 1$	—	0.603				

[a] A ($\theta = 1$) CO absorbance on adsorption of 10 Torr CO for 10 min at 298 K; $A(D,o)$ = absorbance of desorptive CO before resumed CO adsorption; $A(D)$ = calculated absorbance of desorptive CO on production of CO ir doublet, referred to original baseline.

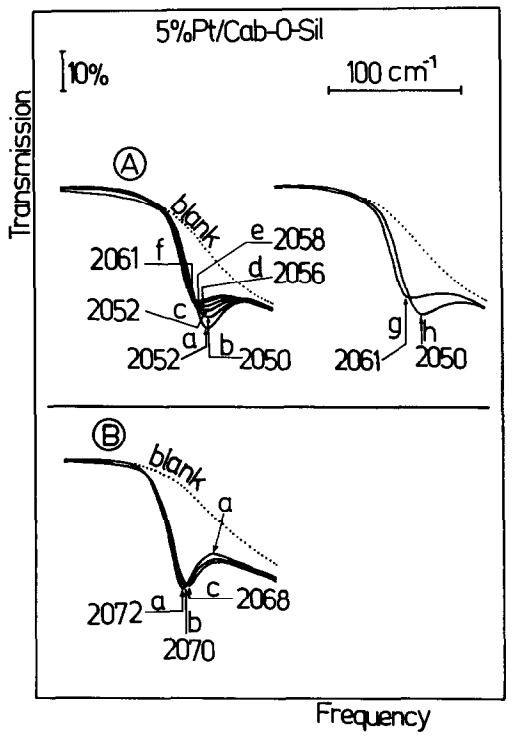

FIG. 2. (A) Effect of H_2 at 298 K on desorptive CO produced as in Fig. 1C: (*a*) desorptive CO [relative to maximum CO absorbance, θ_{CO} (A) ≈ 0.21]; followed by H_2 admission (Torr); (*b*) 7.5×10^{-3}; (*c*) 3.75×10^{-2}; (*d*) 7.5×10^{-2}; (*e*) 3.75; and (*f*) 10; (*g*) same as (*f*); (*h*) 10-min evacuation at 298 K. (B) Effect of H_2 at 298 K on adsorptive CO: (*a*) adsorptive CO [θ_{CO}(B) ≈ 0.24]; followed by (*b*) 10 Torr H_2 for 10 min, and (*c*) 100 Torr H_2 for 60 min.

to occur in the surface layer of supported Pt if the catalyst is treated in O_2 at a higher temperature, or if CO + O_2 reaction cycles are performed on the surface (*2–5*). The surface oxide(s) formed react with H_2 during the standard pretreatment at 673 K. However, the structure of this Pt surface in all probability differs from that existing before the CO + O_2 cycles. Figure 3 demonstrates that a well-resolved CO ir doublet could not be produced on such a Pt/SiO_2 surface, even at various initial desorptive CO absorbances.

4. *Role of Oxygen in Production of CO ir Doublet*

If the process of CO adsorption was in-

TABLE 2

Effect of H_2 on Desorptive and Adsorptive CO on 5% Pt/Cab-O-Sil at 298 K

Catalyst No.	Experimental conditions	Spectra of Figs. 1 and 2		Absorbance $A = \log(T_0/T)_{max}$	Frequency (cm^{-1})
1	Desorptive CO without H_2, then H_2 added (Torr)	2A	(*a*)	0.153	2052
	7.5×10^{-3}		(*b*)	0.123	2050
	3.75×10^{-2}		(*c*)	0.115	2052
	7.50×10^{-2}		(*d*)	0.111	2056
	3.75		(*e*)	0.114	2058
	10		(*f*) or (*g*)	0.115	2061
	Evacuation for 10 min at 298 K		(*h*)	0.130	2050
1	Adsorptive CO without H_2, then H_2 added (Torr)	2B	(*a*)	0.179	2072
	3.0×10^{-2}		—	0.176	2071
	7.5×10^{-2}		—	0.172	2071
	7.5×10^{-1}		—	0.170	2070
	10		(*b*)	0.165	2069
	100		(*c*)	0.157	2068
	Evacuation for 10 min at 298 K		—	0.168	2070
1	Standard pretreatment; 10 Torr H_2 adsorption for 10 min at 298 K; then evacuation for 10 min at 298 K. Followed by CO adsorption (Torr) at 298 K				
	7.5×10^{-3}		—	0.114	2070
	1.5×10^{-2}		—	0.178	2071
	3.0×10^{-2}		—	0.297	2072
	$10(\theta_{CO} \approx 1)$		—	0.579	2079
1	H_2 admission at 298 K into desorptive CO; then evacuation at 298 K [see Fig. 2B, spectrum (g)] and CO admission (Torr)	1D	(*a*)	0.130[a]	2050[a]
	3.75×10^{-3}		(*b*)	0.158	2054
	3.75×10^{-3} (twice)		(*c*)	0.177[b]	2059[b]
	3.75×10^{-3} (3 times)		(*d*)	0.238	2070
	Evacuation at 298 K for 10 min	1E	(*a*)	0.257	2071
	Evacuation at 333 K for 5 min		—	0.258	2071
	Evacuation at 373 K for 5 min		(*f*)	0.272	2071
	Evacuation at 398 K for 5 min	1F	(*g*)	0.278	2068
	Evacuation at 433 K for 5 min		(*h*)	0.283	2063

[a] Data on desorptive CO.
[b] Data from this point on adsorptive CO.

terrupted at 298 K, and continued after the admission of a small amount of oxygen, a shoulder peak was also transiently recorded at 2078–2080 cm^{-1} (Fig. 4A, spectra *c* and *d*) until the CO had reacted with the adsorbed oxygen (spectrum *e*).

A study was next made of the effect of oxygen on the possibility of producing the CO ir doublet. Desorptive CO was prepared as in Fig. 1C. However, there was a small (constant) leak in the sealing of one of the NaCl windows at the bottom of the ir cell in this experiment so that during evacuation at 298 K during the time to record one spectrum (ca. 2.5 min) the intensity of the CO band decreased by an absorbance value

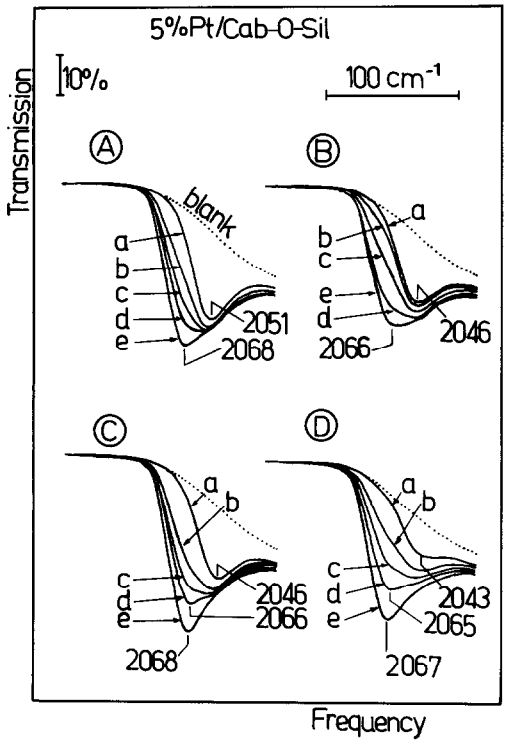

FIG. 3. Attempts to produce CO ir doublet on sample used in 5 CO–O_2 reaction cycles. Treatment: after standard pretreatment, in 100 Torr O_2 for 5 min each at 298, 423, 473, 573, or 673 K, then cooling to 298 K in O_2, and evacuation for 10 min; admission of 10 Torr CO onto the sample at 298 K, for 5 min in each case. Subsequently, pretreatment in O_2 and in H_2 in the normal way at 673 K before each experiment (A, B, C, or D). (*a*) Desorptive CO—absorbances: 0.155 (A), 0.114 (B), 0.120 (C), and 0.060 (D) (for their production see Fig. 1C); from (*b*) to (*f*) stepwise CO adsorption at 298 K until appropriate CO absorbances.

of 5.6×10^{-3} (in our case, at a transmittance of 54%, this decrease was ca. 0.7%). Therefore, during the preparation of desorptive CO a small amount of oxygen also reached the Pt surface (which may have changed the surface structure or/and formed oxide in part). As seen in Fig. 4B, even with very small admissions of CO, the CO ir doublet could be produced with very good resolution of this surface. The small amount of oxygen seeping in continuously decreased the intensity of the desorptive CO band too (Fig. 4B, spectra *e* and *f*). A separate study was made of the effect of O_2 on the CO doublet.

5. *Interaction of O_2 at 298 K with Surface CO giving CO ir Doublet*

The CO ir doublets were produced in accordance with Figs. 1A or C, and the pressure of O_2 in the well-sealed ir cell was then progressively raised at 298 K. In both cases the first O_2 doses were accompanied by decreases in transmittance of the adsorptive CO band (by 0.7 and 0.5%, respectively), while the intensity of the desorptive CO band fell (Fig. 5). After the total disappearance of the adsorptive CO band, however, there was a well-observable decrease in the intensity of the adsorptive CO band, and in parallel with this in its frequency too. As the O_2 pressure was increased, there was a

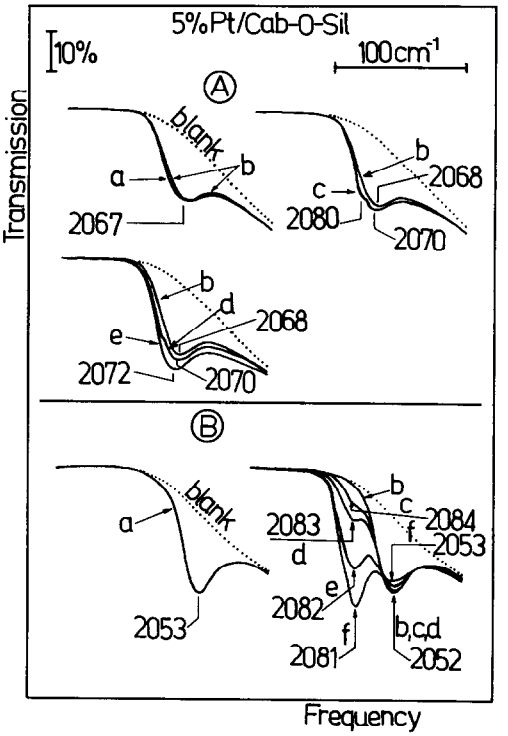

FIG. 4. (A) Effect of O_2 on process of CO adsorption at 298 K on reduced sample (by standard pretreatment). (*a*) 10^{-4} Torr CO, then evacuation for 5 min (adsorptive CO); (*b*) two admissions of 5×10^{-4} Torr O_2, a 1-min waiting period, and evacuation for 5 min; (*c*)–(*e*) continuation of CO adsorption. (B) Effect of O_2 on formation of CO ir doublet: (*a*) desorptive CO + small amount of O_2 (see text); (*b*) as in (*a*), but 2.5 min later; (*c*)–(*f*) stepwise CO adsorption at 298 K until appropriate absorbance of adsorptive CO.

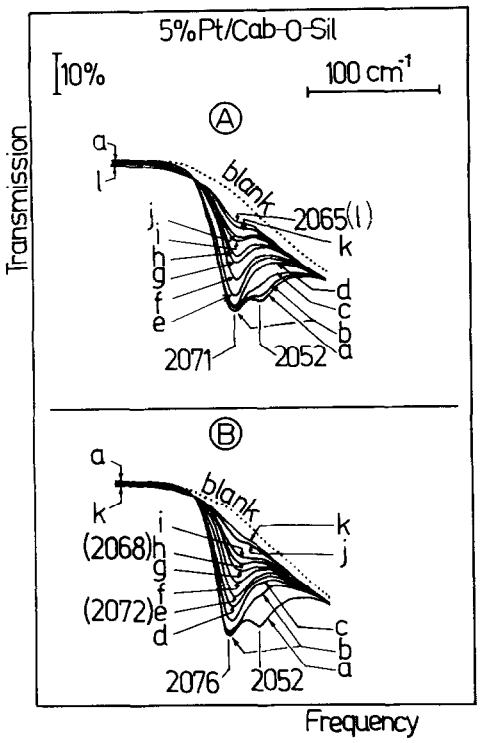

FIG. 5. Interaction of O_2 at 298 K with surface CO layers relating to CO ir doublet. Production of the latter: (A) as in Fig. 1; (B) as in Fig. 1C. O_2 was next admitted (Torr): (A)—(*a*) no O_2; (*b*) 1.5×10^{-3}; (*c*) 7.5×10^{-3}; (*d*) 9×10^{-3}; (*e*) 1.5×10^{-2}; (*f*) 3×10^{-2}; (*g*) 5.25×10^{-2}; (*h*) 7.5×10^{-1}; (*i*) 1; (*j*) 2; (*k*) 5; and (*l*) 10. (B)—(*a*) no O_2; (*b*) 7.5×10^{-3}; (*c*) 1.5×10^{-2}; (*d*) 3×10^{-2}; (*e*) 3.75×10^{-2}; (*f*) 7.5×10^{-2}; (*g*) 3.75×10^{-1}; (*h*) 7.5×10^{-1}; (*i*) 1.5; (*j*) 5; and (*k*) 10.

slight fall in the transmittance of the baseline (2% at 10 Torr O_2), due to the adsorbed oxygen. With the decrease of the CO coverage, the reactivity of the adsorptive CO fell.

DISCUSSION

(A) Formation of CO ir Doublet

1. Formal explanation. There is a good separation of the adsorptive and desorptive CO bands if the frequency difference between them is fairly large, if the half-widths of the bands are sufficiently small, and if the bands (particularly that of adsorptive CO) display minimum asymmetry. Under our experimental conditions (at constant instrumental parameters) oxygen increased the frequency difference between the two bands, while hydrogen decreased it. The half-width and asymmetry of the adsorptive CO band were decreased appreciably by coadsorbed oxygen and to a slight extent by surface treatment in CO at higher temperature, while they were increased by hydrogen. This would give a formal explanation for some of the results shown in Figs. 1, 3, and 4. However, it is obvious that deeper conclusions cannot be drawn merely on the basis of these aspects.

2. Adsorption–Desorption Hysteresis—Surface Heterogeneity—Stratification—CO ir Doublet

To get a better understanding, we have to consider the processes occurring during CO adsorption–thermodesorption on a self-supporting 5% Pt/Cab-O-Sil tablet. Supported catalysts differ in many respects from large single crystals and metal ribbons. In the thick (100–110 μm) Pt/SiO_2 used, the calculated average metal particle size was 2.4 nm (sample 1) or 2.8 nm (sample 2); since the interaction between Pt and SiO_2 is negligible, the use of terraces, steps, and kinks is allowed in the evaluation of the ir spectra (*6*).

The CO ir doublet was produced on the basis of the adsorption–desorption hysteresis in ν(CO) as a function of θ_{CO}, which is particularly large (20–30 cm^{-1}) for supported Pt (*1, 2*), but it was also observed on Pt ribbon with (111) orientation (*7*). The hysteresis was attributed to the lack of thermodynamic equilibrium ($T \leq 300$ K) (*7a*), and later mainly to surface defects or steps (*7b*). When the number of the latter was decreased, the magnitude of the hysteresis diminished (from ca. 11 to 3 cm^{-1}) (*7b*). Accordingly, the much higher concentration of steps, kinks, and other defect sites on Pt/SiO_2 should be at least one of the reasons to observe a higher extent of hysteresis.

The adsorption heat and sticking coefficient of CO (s_{CO}) are high on Pt surfaces with either small or large Miller indices (*7a,*

8–10). If a CO molecule from the gas phase collides with a free Pt surface at 298 K, there is a high probability that it will be adsorbed. This has two consequences: (i) Microscopic aspects: During the energy-loss process of adsorption, surface migration over various distances may occur, depending on the surface heterogeneity and on the adsorbed surface layer (*11*). CO will be located at lower coverages not only on the energetically most favored sites (steps, kinks), but elsewhere too (on terraces), depending on their surface magnitudes. (ii) Macroscopic aspects: However, the locations of the individual Pt crystallites inside the tablet are also important. The stepwise CO adsorption at 298 K on a self-supporting 5% Pt/Cab-O-Sil may take place in a nonuniform distribution (stratification) (*12, 13*). This process may also cause an increase in ν(CO) for the adsorption branch of the hysteresis.

Considering (*8, 9, 11–19*), at increasing temperature, an activation energy-requiring surface migration (intraparticular diffusion) and/or desorption–readsorption (interparticular diffusion) occur, depending on the location and/or on the local coverage of CO on the Pt crystallites. This results in a more uniform CO distribution (Fig. 6). However, after a certain degree of thermodesorption and after cooling the sample to room temperature, the CO remaining on the Pt surface (desorptive CO) is found microscopically predominant on steps and kinks

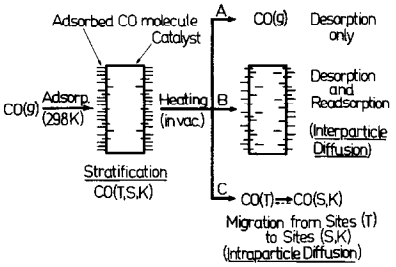

FIG. 6. Summary of main processes occurring at relatively low average θ_{CO} on adsorption of CO at 298 K on 5% Pt/Cab-O-Sil in a static ir cell, and on moderate heat treatment of the adlayer under vacuum.

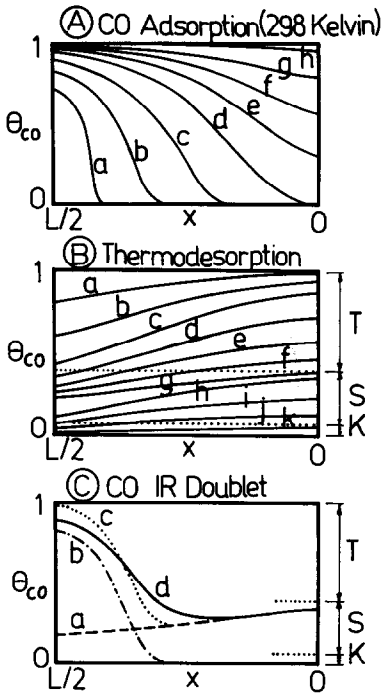

FIG. 7. A qualitative conception for the variations of $\theta_{CO,local}$ in the interior of a self-supporting 5% Pt/SiO_2 sample: (A) during stepwise CO adsorption at 298 K (from *a* to *h*); (B) during desorption by progressive temperature increase under vacuum after $\theta_{CO} = 1$ (from *a* to *k*); and (C) following production of CO ir doublet: separately produced (*a*) desorptive CO, and (*b*) adsorptive CO; (*c*) sum of (*a*) and (*b*); and (*d*) production of CO ir doublet. x = distance from center of sample; L = sample thickness; T, S, and K = assumed relative proportions of adsorption sites on terraces, steps, and kinks (other defect sites neglected).

(defect sites) as was assumed in (*1*). We have given a qualitative picture of the CO distribution inside the sample under the stepwise adsorption, thermodesorption, and production of the CO ir doublet (Fig. 7).

During CO adsorption at 298 K, the steepness of the CO concentration profile in a sample, and consequently (more or less) the possibility of production of the CO ir doublet, are determined by the relative rate of CO adsorption ($r_{ads,CO}$) compared to the gas-phase diffusion of CO ($r_{g.diff,CO}$) from the outside toward the center of the sample. $r_{g.diff,CO}$ varied during a run as the CO

pressure was gradually changed through it. However, the conditions of $r_{g.diff,CO}$ may be taken as identical, or only slightly different in the corresponding parts (sections) of each experiment. The exception may be the results in Figs. 1D and 4B, where the H_2 or CO_2 released inside the sample might have had a slight influence on $r_{g.diff,CO}$ (increase or decrease). $r_{ads,CO}$ is influenced by s_{CO} on bare Pt and on Pt surfaces partially covered by CO or/and coadsorbed substance(s).

For the interpretation of the results in Fig. 3, it may be assumed that the Pt surface became "smoother," the surface mobility of CO increased, and s_{CO} slightly decreased. This suggests that the differences to be seen in Figs. 1A and B might be explained in that the surface heterogeneity of the Pt could still increase during standard pretreatments, resulting in a better resolution of the CO ir doublet.

s_{CO} and hence the extent of stratification too should decrease during the replacement of preadsorbed H by CO (Fig. 1D), which would explain in part the differences in the shapes of the adsorptive CO ir bands to those in Figs. 1A and B. However, at 298 K H_2 almost totally eliminated the resolution of an already existing CO ir doublet (*1*), and the adsorptive and desorptive CO layers showed differences in response to H_2. Consequently, an important role must also be ascribed to the interaction of H(ads) and CO(ads) on Pt in Figs. 1D–F (see below).

During pretreatment in CO (Fig. 1C), some CO molecules could have dissociated to C and O atoms on the steps and kinks (*15*). By analogy with the results on sulfur-contaminated stepped Pt single crystals (*18*), it may be assumed that the surface C atoms decreased s_{CO} on these sites, but did not decrease it much on the terraces. However, during production of the CO ir doublet, the ordering of the adsorptive CO layers might be impeded by these small amounts of immobile surface C (*20*) or/and by the additional surface defect sites produced by CO-induced imperfect ordering of Pt atoms during CO pretreatment (*21*). This might explain why the frequency of the adsorptive CO was higher, and the asymmetry of its ir band and consequently the value of $A(D)/A(D,o)$ (Table 1) were lower, i.e., the resolution of the CO ir doublet improved.

(B) Interaction of CO with O_2 and H_2—Surface Heterogeneity—Local Surface CO Concentration

When the CO adsorption was interrupted and a small amount of O_2 was then admitted at 298 K onto the adsorptive CO, only a very slight reaction occurred (Fig. 4A, spectra *a* and *b*). The adsorptive CO characterized by a high enough $\theta_{CO,local}$ inhibited the dissociative adsorption of O_2 on the outer part of the tablet (*22*). Thus, the remaining O_2 was adsorbed on the empty, deeper-lying layers of the sample; mainly on steps and kinks, because of the much higher sticking coefficient of O_2 on these sites (*14, 23, 24*). When CO adsorption was resumed at 298 K, the O(ads) + CO(g) process took place on the surface sites in question, which resulted in a CO band at higher frequency (*2*) here as a shoulder until the CO had reacted with the O(ads) (Fig. 4A, spectra *c* and *d*). When O_2 came into contact with the Pt surface at higher temperature (Fig. 4B), a surface transition might take place and some Pt oxide might also form, but below the detection limit (the band at 2120 cm^{-1} was not observable during CO adsorption). According to previous results (*2*), this caused a higher frequency of the adsorptive CO and consequently, a well-resolved ir doublet.

The results in Fig. 5 can similarly be interpreted on the basis of: (a) the features of the adsorptive and desorptive CO, and (b) the preferential adsorption properties of O_2. The transient increase in the intensity of the adsorptive CO (spectrum *b*) was attributed to the migration of some CO molecules from the steps to the terraces caused by the adsorption of the first O_2 doses. However, although the reactivity of CO(ads) decreased with the progress of the

surface reaction, the sequence of reactivity toward O_2 for adsorptive CO and desorptive CO (Fig. 5) is inconsistent with the results mentioned in (*1*). These contradictions were attributed to the possibility of the different crystal structures of the samples in (*1*) and in this study (e.g., more steps here).

Although hydrogen is also bound more strongly on bare Pt steps than on terraces (*25–28*), and s_H too is higher in the presence of steps than in their absence (*26*), the mobility of the H(ads) atoms on Pt is so great that s_H cannot be measured separately on the steps and terraces (*28*). Tanaka and White (*29*) suggested two forms of CO adsorbed (on terraces and on steps) on Pt/TiO_2. They proposed, however, that the bulk of CO molecules on Pt was mobile at 298 K, and that some CO migrated from the steps to the terraces caused by hydrogen coadsorption on the steps.

If this process is also accepted for Pt/SiO_2, in principle we would obtain an explanation for the ν(CO) increase and intensity decrease to be seen in Fig. 2A. However, ν(CO) increased only at higher H_2 pressures (from 10^{-2} to 10 Torr) and without any new band or at most a shoulder at higher frequency, and ν(CO) decreased so much on evacuation at 298 K for Pt/SiO_2 that we question the acceptance of CO migration from the steps to the terraces on hydrogen treatment. On the basis of work function measurements, it was suggested (*26*) that the H atom was attached by a covalent bond to bare Pt, but that on the terraces H(ads) had a slight δ^+ charge, while on the steps (in the vicinity of the steps) it had a δ^- charge. Thus, H(ads) on the steps decreased the metal electron concentration, whereas that on the terraces increased it. If it is assumed that the electronic properties of H(ads) to a first approximation remained similar (but at least was not opposite) when coadsorption with CO took place, then according to the $d \rightarrow 2\pi^*$ electron back-donation model and long-range effect (*3, 30*) the transitional red shift in the frequency of desorptive CO (Fig. 2A, *b*) might be attributed to the H(ads)$^{\delta+}$ on the empty terraces. However, the CO molecules located mainly on the steps and kinks (desorptive CO) hindered hydrogen adsorption on these sites. Accordingly we presumed that (a) the desorptive CO and hydrogen interacted on the steps/kinks in such a way that the strength of the PtC–O bond increased and that of Pt–hydrogen decreased, and (b) the effect of adsorbed hydrogen on desorptive CO on steps was greater than that H(ads) on terraces. This was why we observed the blue shift in ν(CO) only at higher H_2 pressures and why the hydrogen causing this effect could be evacuated at 298 K. The electron-attracting property of H(ads) on Ni was also used to interpret the frequency increase (from 2040 to 2070 cm^{-1}) of CO on Ni/SiO_2 (*31*). Recently, repulsive or attractive interactions were proposed (*32*) between CO(ads) and H(ads) on closed or open crystal faces, and the blue shift in the ν(CO) of the linearly adsorbed CO on Ni(100) due to H(ads) was similarly explained by an increase of the NiC–O bond strength (*32c*). Jiehan *et al.* (*33*) also observed a ν(CO) increase on Pt/TiO_2 treated in H_2, but they interpreted this in terms of the interaction of CO(ads) and H(ads) (probably protons) originating from the TiO_2. However, it is probable that this back-spillover process is not acceptable for Pt/SiO_2.

For adsorptive CO + H_2, or preadsorbed hydrogen + CO (Fig. 2B, Table 2), the hydrogen could not have a large effect on CO(ads). A small red shift was observed only in ν(CO), since the local CO coverage was high enough and the geometrical structure of the CO(ads) layer was different from that for desorptive CO.

CONCLUSIONS

(1) The possibility of producing the CO ir doublet on Pt/Cab-O-Sil depended on the Pt surface and on the other substances on the surface.

(2) The possibility of producing this dou-

blet may be determined fundamentally by (a) the adsorption and desorption properties of the various Pt crystal faces (terraces, steps, kinks), and the limited surface CO migration, and/or (b) the nonuniform distribution of CO in a self-supporting Pt/Cab-O-Sil sample at lower average CO coverages at room temperature.

(3) The surface CO layers pertaining to the CO ir doublet exhibited different reactivities toward oxygen, and differences were also exhibited by the interactions of the separately examined adsorptive CO and desorptive CO with hydrogen at 298 K.

(4) In these interactions, the surface heterogeneity, the different adsorption properties of O_2 and H_2, and the local surface CO concentration with different surface structures might play important roles.

REFERENCES

1. Bartók, M., Sárkány, J., and Sitkei, A., *J. Catal.* **72,** 236 (1981).
2. Sárkány, J., Bartók, M., and Gonzalez, R. D., *J. Catal.* **81,** 347 (1983).
3. Primet, M., Basset, J. M., Mathieu, M. V., and Prettre, M., *J. Catal.* **29,** 213 (1973).
4. Heyne, H., and Tompkins, F. C., *Trans. Faraday Soc.* **63,** 1274 (1967).
5. Shigeishi, R. A., and King, D. A., *Surf. Sci.* **75,** L397 (1978).
6. Sheppard, N., and Nguyen, T. T., *in* "Advances in Infrared and Raman Spectroscopy" (R. Hester and R. J. H. Clark, Eds.), Vol. 5, p. 67. Heyden and Son, London, 1978.
7. (a) Shigeishi, R. A., and King, D. A., *Surf. Sci.* **58,** 379 (1976); (b) Crossley, A., and King, D. A., *Surf. Sci.* **68,** 528 (1977); **95,** 131 (1980).
8. Campbell, C. T., Ertl, G., Kuipers, H., and Segner, J., *Surf. Sci.* **107,** 207 (1981).
9. Lin, T. H., and Somorjai, G. A., *Surf. Sci.* **107,** 573 (1981).
10. Bredén, G., Pirug, G., and Bonzel, H. P., *Surf. Sci.* **72,** 45 (1978).
11. King, D. A., *J. Vac. Sci. Technol.* **17,** 241 (1980).
12. (a) Eischens, R. P., *Acc. Chem. Res.* **5,** 74 (1972); (b) Palazov, A., Chang, C. C., and Kokes, R. J., *J. Catal.* **36,** 338 (1975).
13. Primet, M., *J. Catal.* **88,** 273 (1984).
14. Poelsema, B., Palmer, R. L., and Comsa, C., *Surf. Sci.* **123,** 152 (1982) and references therein.
15. Iwasawa, Y., Mason, R., Textor, M., and Somorjai, G., A., *Surf. Sci.* **44,** 468 (1976).
16. Norton, P. R., Coodale, J. W., and Selkirk, B. B., *Surf. Sci.* **83,** 189 (1979).
17. McClellan, M. R., Gland, J. L., and Feeley, F. R., *Surf. Sci.* **112,** 63 (1981).
18. Gdowski, G. E., and Madix, R. J., *Surf. Sci.* **115,** 524 (1982).
19. (a) Herz, R. K., Kiela, J. B., and Martin, S. P., *J. Catal.* **73,** 66 (1982); (b) Lee, P. I., and Schwarz, J. A., *J. Catal.* **73,** 272 (1982); (c) Gorte, R. J., *J. Catal.* **75,** 164 (1982); (d) Jones, D. M., and Griffin, G. L., *J. Catal.* **80,** 40 (1983); (e) Falconer, J. L., and Schwarz, J. A., *Catal. Rev.-Sci. Eng.* **25,** 141 (1983).
20. Comrie, C. M., and Lambert, R. M., *J. Chem. Soc. Faraday Trans. 1* **72,** 1659 (1976).
21. Hofmann, P. Bare, S. R., and King, D. A., *Surf. Sci.* **117,** 245 (1982).
22. Schwarz, J. A., and Smith, R. D., *J. Catal.* **62,** 176 (1980).
23. Comsa, G., Mechterscheimer, G., and Poelsema, B., *Surf. Sci.* **119,** 172 (1982).
24. Hopster, H., Ibach, H., and Comsa, G., *J. Catal.* **46,** 37 (1977).
25. (a) Collins, D. M., and Spicer, W. E., *Surf. Sci.* **69,** 85 (1977); (b) **69,** 114 (1977).
26. Christmann, K., and Ertl, G., *Surf. Sci.* **60,** 365 (1976).
27. Salmerón, M., Gale, R. J., and Somorjai, G. A., *J. Chem. Phys.* **70,** 2807 (1979).
28. Poelsema, B., Mechterscheimer, G., and Comsa, G., *Surf. Sci.* **111,** 519 (1981).
29. Tanaka, K., and White, J. M., *J. Catal.* **79,** 81 (1983).
30. (a) Blyholder, G., *J. Phys. Chem.* **68,** 2772 (1964); (b) Blyholder, G., *J. Phys. Chem.* **79,** 756 (1975).
31. Primet, M., and Sheppard, N., *J. Catal.* **41,** 258 (1976).
32. (a) Peebles, D. E. Creighton, J. R., Belton, D. M., and White, J. M., *J. Catal.* **80,** 482 (1983); (b) Koel, B. E., Peebles, D. E., and White, J. M., *Surf. Sci.* **125,** 709 (1983); **125,** 739 (1983); (c) Mitchell, G. E., Gland, J. L., and White, J. M., *Surf. Sci.* **131,** 167 (1983).
33. Jiehan, H., Zupei, H., Yongze, S., and Hongli, W., *Stud. Surf. Sci. Catal.* **17,** 53 (1983).